Available online at www.sciencedirect.com
SCIENCE DIRECT®
C. R. Mecanique 334 (2006) 373–379
COMPTES RENDUS MECANIQUE
http://france.elsevier.com/direct/CRAS2B/

Estimation of the mesoscopic thermoplastic dissipation in High-Cycle Fatigue

Eric Charkaluk [a,*], Andrei Constantinescu [b]

[a] *Laboratoire de mécanique de Lille – CNRS UMR 8107, boulevard Paul-Langevin, 59655 Villeneuve d'Ascq cedex, France*
[b] *Laboratoire de mécanique des solides – CNRS UMR 7649, École polytechnique, 91128 Palaiseau cedex, France*

Received 27 March 2006; accepted 28 March 2006

Available online 15 May 2006

Presented by Huy Duong Bui

Abstract

A series of High-Cycle Fatigue (HCF) criteria for polycrystalline materials is based on a multiscale interpretation, proposed initially by Dang Van, in which the principal concepts are a two scales model and a shakedown condition. The purpose of this Note is to extend the study of the different dissipative regimes during cyclic loading within this framework by using a self consistent homogenization scheme in coupled thermoplasticity. It is shown that the Sachs and Lin-Taylor schemes are not able to represent the thermal evolutions observed during fatigue tests. ***To cite this article: E. Charkaluk, A. Constantinescu, C. R. Mecanique 334 (2006).***
© 2006 Académie des sciences. Published by Elsevier SAS. All rights reserved.

Résumé

Estimation de la dissipation thermoplastique en fatigue à grand nombre de cycles. Les critères de fatigue à grand nombre de cycles pour matériaux polycristallins fondés sur une interprétation multiéchelles, initiés par Dang Van, sont développés à partir de deux concepts : un modèle à deux échelles et une condition d'adaptation. L'objectif de cette Note est d'étendre l'étude des différents régimes dissipatifs sous sollicitations cycliques dans ce cadre en utilisant un schéma d'homogénéisation autocohérent en thermoplasticité couplée. Il est montré que les schémas de Sachs et Lin-Taylor ne sont pas capables de représenter les évolutions thermiques observées durant des essais de fatigue. ***Pour citer cet article : E. Charkaluk, A. Constantinescu, C. R. Mecanique 334 (2006).***
© 2006 Académie des sciences. Published by Elsevier SAS. All rights reserved.

Keywords: Fatigue; Dissipation; Micromechanics; Self-consistent scheme

Mots-clés : Fatigue ; Dissipation ; Micromécanique ; Schéma autocohérent

* Corresponding author.
E-mail addresses: eric.charkaluk@univ-lille1.fr (E. Charkaluk), andrei.constantinescu@lms.polytechnique.fr (A. Constantinescu).

1631-0721/$ – see front matter © 2006 Académie des sciences. Published by Elsevier SAS. All rights reserved.
doi:10.1016/j.crme.2006.03.014

1. Introduction

A series of High-Cycle Fatigue (HCF) criteria for polycrystalline materials is based on a mesoscopic-macroscopic interpretation of dissipative phenomena. Let us recall shortly the main results.

Dang Van, followed by Papadopoulos (see, for example, [1]) postulated that fatigue is initiated through plastic shakedown of misoriented grains after a complex damaging mechanism. Their model represents the misoriented grain as a plastic inclusion in an infinite elastic matrix under the Lin-Taylor homogenization assumption [2] to relate the macroscopic elastic fields and the mesoscopic elastoplastic fields. The fatigue limit, corresponding to infinite lifetimes, is therefore obtained as a shakedown limit by using the shakedown theorem in Mandel's formulation [3].

The elastic shakedown limit can be associated with a bounded dissipated energy. This has recently been formally expressed by Nguyen [4] and observed experimentally by infrared thermography by Luong [5] and later, among others, by Fargione et al. [6]. The observed regimes are: a quasi-non dissipative one, when the applied load is under the macroscopic fatigue limit, and a highly dissipative one, when cyclic loading is beyond this limit. This experimental approach was recently explored by Boulanger [7] and Doudard [8,9].

The objective of the present Note is to explore the meso-macro passage proposed by Dang Van and Papadopoulos from the dissipative point of view. The work is based on the development of a generalised self-consistent scheme as in Cano et al. [10], expressed here in the framework of coupled thermoplasticity. The analysis shows that the Lin-Taylor or the Sachs homogenization assumptions do not conduct to the observed thermal evolutions, whether Kröner's assumption conducts to qualitative match.

The paper presents in the next section the thermodynamical framework and its relation with the macro-meso homogenisation schemes. The third section discusses the form of the heat balance equation obtained for each homogenisation scheme. The obtained heat equation is then numerically integrated using parameters from literature and the results are discussed in the final section.

2. The thermomechanical framework

The thermomechanical analysis of the deformation of continuum bodies can be structured using the framework of continuum thermodynamics of irreversible processes (TIP) [11]. For the necessary assumptions on meso- and macroscopic energies, one can consult the presentation given by Doudard [8,9]. The main purpose of this section is the construction of a thermomechanically coupled heat balance equation.

We shall first recall the multiscale framework proposed by Dang Van and Papadopoulos in HCF. The misoriented grain is considered as a plastic inclusion embedded in an infinite elastic matrix. Let denote by $\boldsymbol{\Sigma}$ and $\boldsymbol{E}$ the macroscopic elastic stress and strain tensors, respectively and by $\boldsymbol{\sigma}$, $\boldsymbol{\varepsilon}$ and $\boldsymbol{\varepsilon}^p$ the mesoscopic stress, strain and respectively plastic strain tensors.

Helmoltz's free energy Ψ, can be additively splitted in the free energy of the plastic inclusion Ψ_{in} and of the elastic matrix Ψ_{mat}:

$$\Psi = f_v \cdot \Psi_{\text{in}} + (1 - f_v) \cdot \Psi_{\text{mat}}$$

where f_v denotes the volumic ratio of the plastic inclusions.

Let us assume that the mesoscopic specific free energy in the inclusion Ψ_{in} only depends on the temperature T and the mesoscopic strain fields $\boldsymbol{\varepsilon}^e$ and $\boldsymbol{\varepsilon}^p$. The macroscopic free energy in the matrix Ψ_{mat} only depends on temperature T and the macroscopic strain field $\boldsymbol{E}$:

$$\Psi_{\text{in}} = \Psi_{\text{in}}\big(T, \boldsymbol{\varepsilon}^e, \boldsymbol{\varepsilon}^p\big), \qquad \Psi_{\text{mat}} = \Psi_{\text{mat}}(T, \boldsymbol{E})$$

Under the assumption of a linear isotropic thermoelastic matrix, the free energy Ψ_{mat} has the following form:

$$\rho\Psi_{\text{mat}}(T, \boldsymbol{E}) = \frac{1}{2}\big(\lambda \operatorname{tr}(\boldsymbol{E})^2 + 2\mu \operatorname{tr}\big(\boldsymbol{E}^2\big)\big) - (3\lambda + 2\mu)\alpha\theta \operatorname{tr}(\boldsymbol{E}) + \frac{C_v\theta^2}{2T_0}$$

where $\theta = T - T_0$, λ and μ are the Lamé coefficients, C_v is the specific heat capacity and α is the thermal expansion coefficient. Following Papadopoulos [1], a linear kinematic hardening rule for the plastic inclusion at the mesoscopic scale can be chosen and the following assumption on the free energy Ψ_{in} is taken:

$$\rho\Psi_{\text{in}}\big(T, \boldsymbol{\varepsilon}^e, \boldsymbol{\varepsilon}^p\big) = \frac{1}{2}\big(\lambda \operatorname{tr}\big(\boldsymbol{\varepsilon}^e\big)^2 + 2\mu \operatorname{tr}\big(\boldsymbol{\varepsilon}^{e2}\big)\big) - (3\lambda + 2\mu)\alpha\theta \operatorname{tr}\big(\boldsymbol{\varepsilon}^e\big) + \frac{1}{3}c \operatorname{tr}\big(\boldsymbol{\varepsilon}^{p2}\big) + \frac{C_v\theta^2}{2T_0}$$

where c is the kinematic hardening modulus.

The second law of thermodynamics conducts classically to the following relations between the state variables $\boldsymbol{E}$, $\boldsymbol{\varepsilon}^e$ and $\boldsymbol{\varepsilon}^p$ and the dual variables, also denoted as associated thermodynamical forces, $\boldsymbol{\Sigma}$, $\boldsymbol{\sigma}$ and $\boldsymbol{a}$:

$$\boldsymbol{\Sigma} = \rho \frac{\partial \Psi_{\text{mat}}}{\partial \boldsymbol{E}}, \qquad \boldsymbol{\sigma} = \rho \frac{\partial \Psi_{\text{in}}}{\partial \boldsymbol{\varepsilon}^e}, \qquad \boldsymbol{a} = \rho \frac{\partial \Psi_{\text{in}}}{\partial \boldsymbol{\varepsilon}^p}$$

Taking into account the chosen expression of the free energies in the expression of the first law of thermodynamics, the heat balance equation is written as:

$$\begin{aligned} \rho C_v \dot{\theta} = {} & r + \operatorname{div}(\boldsymbol{k} \operatorname{grad} \theta) + \boldsymbol{\Sigma} : \dot{\boldsymbol{E}} - (1 - f_v)\big(\boldsymbol{\Sigma} : \dot{\boldsymbol{E}} + \alpha\theta \operatorname{tr}\big(\dot{\boldsymbol{\Sigma}}\big) + 9K\alpha^2\theta\dot{\theta}\big) \\ & - f_v\big(\boldsymbol{\sigma} : \dot{\boldsymbol{\varepsilon}}^e + \boldsymbol{a} : \dot{\boldsymbol{\varepsilon}}^p + \alpha\theta \operatorname{tr}(\dot{\boldsymbol{\sigma}}) + 9K\alpha^2\theta\dot{\theta}\big) \end{aligned} \tag{1}$$

where $3K = 3\lambda + 2\mu$ denotes the isotropic compression moduli and $\boldsymbol{k}$ denotes the second rank tensor of conductivities.

In fact, given the expression of the free energies, the heat equation (1) and the balance of forces, the equations governing the thermomechanical system are completed provided the relation between macroscopic and mesoscopic fields is specified.

3. The heat balance equation and the homogenization schemes

In the present context of a plastic inclusion in an elastic matrix, the relations between mesoscopic and macroscopic fields can be reached, for example, using one of the following homogenization assumptions (see, for example, Cano [10]):

- *Lin-Taylor* supposes strain equality: $\boldsymbol{\varepsilon} = \boldsymbol{E}$. This is the hypothesis of the initial Dang Van or Papadopoulos fatigue criterion.
- *Sachs* supposes stress equality: $\boldsymbol{\sigma} = \boldsymbol{\Sigma}$.
- *Kröner* assumes:

  $$\boldsymbol{\sigma} = \boldsymbol{\Sigma} - \mathbb{C} : (\mathbb{I} - \mathbb{P} : \mathbb{C}) : \boldsymbol{\varepsilon}^p$$

  where $\mathbb{C}$ and $\mathbb{P}$ are respectively the fourth rank elastic moduli and Hill tensors. In the particular case of an idealized spherical inclusion, $\mathbb{P}$ reads:

  $$\mathbb{P} = \frac{a}{3K}\mathbb{J} + \frac{b}{2\mu}\mathbb{K}, \quad \text{with } a = \frac{3K}{3K + 4\mu} \text{ and } b = \frac{6}{5}\frac{K + 2\mu}{3K + 4\mu}$$

  where $\mathbb{J} = \frac{1}{3}\boldsymbol{I} \otimes \boldsymbol{I}$ and $\mathbb{K} = \mathbb{I} - \mathbb{J}$ with $\mathbb{I}$ the fourth rank identity tensor.

In all the cases, the same elastic behaviour at the mesoscopic and the macroscopic scale is assumed. Then, the relation between mesoscopic and macroscopic fields can be written in the general form:

$$\boldsymbol{\sigma} = \boldsymbol{\Sigma} - \mathbb{C}^* : \boldsymbol{\varepsilon}^p = \boldsymbol{\Sigma} + \boldsymbol{\rho}^* \tag{2}$$

where $\boldsymbol{\rho}^*$ should be interpreted as a mesoscopic residual stress field.

The particular cases of each model are obtained for the next form of $\mathbb{C}^*$:

- for Lin-Taylor's model, $\mathbb{C}^* = \mathbb{C}$;
- for Sachs model, $\mathbb{C}^* = 0$; and
- for Kröner's scheme, $\mathbb{C}^* = \mathbb{C} : (\mathbb{I} - \mathbb{P} : \mathbb{C})$.

In the case of isotropic elastic behavior with a classically defined deviatoric plasticity, one can remark that:

$$\operatorname{tr}(\boldsymbol{\sigma}) = \operatorname{tr}(\boldsymbol{\Sigma}), \qquad \boldsymbol{\rho}^* = -\mathbb{L}^* : \boldsymbol{\varepsilon}^p = -(2\mu - 2\mu b)\boldsymbol{\varepsilon}^p \tag{3}$$

where $b = 1$ for the Sachs's model and $b = 0$ for the Lin-Taylor's model. In the particular case of a linear kinematic hardening, using the definition of the free energy Ψ_{in}, $\boldsymbol{a} = \frac{2}{3}c\boldsymbol{\varepsilon}^p$. Then, as a consequence of relations (2) and (3), the heat balance equation (1) can be simplified as follows:

$$\rho C_v \dot{\theta} - \operatorname{div}(\boldsymbol{k} \operatorname{grad} \theta) = r + f_v\left(\boldsymbol{\sigma} : \dot{\boldsymbol{\varepsilon}}^p - \frac{2}{3}c\boldsymbol{\varepsilon}^p : \dot{\boldsymbol{\varepsilon}}^p + (2\mu - 2\mu b)\boldsymbol{\varepsilon}^p : \dot{\boldsymbol{\varepsilon}}\right) - \alpha\theta \operatorname{tr} \dot{\boldsymbol{\Sigma}} - 9K\alpha^2\theta\dot{\theta} \tag{4}$$

where heat sources are located on the right side of the previous equation. r is the heat supply and the term $f_v(--)$ is the mechanical power dissipated in the plastic behaviour of the misoriented grains at the mesoscopic scale. We recall that b is a constant depending on the homogenization scheme and that the two last terms express the thermoelastic coupling as a function of the applied macroscopic cyclic loading.

4. Results and discussion for a cyclic tension-compression experiment

4.1. The experiment

Next, we propose to solve the coupled heat equation in the particular case of a tension compression experiment, defined by a macroscopic stress tensor of the form:

$$\boldsymbol{\Sigma} = \Sigma_{11} \sin(\omega t) \boldsymbol{e}_1 \otimes \boldsymbol{e}_1$$

and, in the absence of heat sources, $r = 0$.

We shall assume that the specimen is a thin plate as in Boulanger [7] or Doudard [8], where the conduction phenomenon is isotropic ($\boldsymbol{k} = k\boldsymbol{I}$) and accept, in order to simplify the computations, their estimation of the thermal exchanges associated term (see [15] for more details):

$$-\operatorname{div}(\boldsymbol{k} \operatorname{grad} \theta) \simeq \rho C_v \frac{\theta}{\tau_{\text{eq}}}$$

where τ_{eq} is a constant representative of the heat exchanges with the environment of the specimen through the surface in contact with the air and the grips. This hypothesis is acceptable provided the bulk temperature is considered equal to the surface temperature of the specimen and homogeneous along the surface, and the temperature variations are small.

Then, the heat balance equation (4) can be simplified to:

$$\left(1 + \frac{9K\alpha^2\theta}{\rho C_v}\right)\dot{\theta} - \frac{\theta}{\tau_{\text{eq}}} = \frac{f_v}{\rho C_v}\left(\boldsymbol{\sigma} : \dot{\boldsymbol{\varepsilon}}^p - \frac{2}{3}c\boldsymbol{\varepsilon}^p : \dot{\boldsymbol{\varepsilon}}^p + (2\mu - 2\mu b)\boldsymbol{\varepsilon}^p : \dot{\boldsymbol{\varepsilon}}\right) - \frac{\alpha\theta}{\rho C_v} \operatorname{tr}(\dot{\boldsymbol{\Sigma}}) \tag{5}$$

This equation can easily be integrated provided the mesoscopic plastic strains are determined. They will be computed from the macroscopic loading using the homogenization scheme and a radial-return plastic integration algorithm. A simple numerical integration scheme is given in Appendix A.

It is also important to explain the cyclic technique loading used in this type of experiment, as explained in [5,6,9] Different stress amplitudes are applied on the specimen and each amplitude is maintained until a stabilization of the temperature is observed. The stabilized temperature amplitude is defined as $\theta_{\text{stab}} = T_{\text{stab}} - T_0$. During the tests, one can observe on the one hand side the cyclic variation of temperature, i.e., at each cycle a heating in compression and a cooling in extension as predicted by the thermoelastic coupling (see Fig. 4), and on the other hand a small but continuous growth of the mean temperature due to the plastic dissipation of the misoriented grains.

4.2. The material parameters

In order to integrate numerically the previous equation (5), the material parameters displayed in Table 1 are used. They correspond in large to the ferrite–martensite dual phase steels (DP60 and DP600) as in Boulanger [7] or Doudard [8,9].

ρ, α, C_v, E, ν, τ_{eq} have been deduced from [7–9]. The estimation of the mesoscopic tensile yield stress $\sigma_y =$ 120 MPa is extracted from Monchiet's data [12].

For the plastic hardening bahaviour, a hardening modulus $c = 1000$ MPa has been chosen. The proposed value denotes small distance to a perfect plastic behaviour, which we might have expected as a first approximation. Let us

Table 1
Thermal and mechanical material parameters used for the DP60 steel, after Doudard [8] and Boulanger [7]

ρ (kg m^{-3})	α (K^{-1})	C_v (J kg^{-1} K^{-1})	E (MPa)	ν	a (MPa)	σ_y (MPa)	τ_{eq} (s)
7800	0.00001	460	210 000	0.3	1000	120	80

remark that a perfectly plastic model would not be acceptable for the Sachs model as this would imply under infinite plastic strains as soon as the stress is beyond the yield limit (see Eq. (A.1) with $b = 1$ and $c = 0$).

A delicate point is the estimation of the volumic ratio of plastic inclusions, f_v. The present values are based on a previous work of Cugy and Galtier [13] on low carbon steel. The only available datas are the relative surface covered by slip bands, which can not exactly be correlated to the volumic ratio. A first assumption is to consider this surface ratio as representative of f_v and to take into account the values obtained for low carbon steel. The values observed by Cugy and Galtier are closed to zero near the endurance limit and less than 20% when the stress range is equal to the standard yield stress at 0.2%.

As a consequence, a value of $f_v = 3\%$ is chosen for a stress amplitude of 180 MPa, a value of $f_v = 10\%$ for a stress amplitude of 250 MPa and a value of $f_v = 20\%$ for a stress amplitude of 300 MPa which correspond to the three simulated loadings. Of course this corse assumption has to be refined in future work.

The example discussed next corresponds to tensile fatigue tests at $R_\sigma = -1$, a loading frequency of 50 Hz and stress amplitudes of 180, 250 and 300 MPa, performed by Boulanger [7]. It presents the same qualitative characteristics as results obtained by Luong [5] on a XC55 steel and Fargione et al. [6] on different steels.

First, the macroscopic and mesoscopic stress-strain curves for the different homogenization scheme are compared. In Fig. 1, the results obtained in the case of the Sachs scheme are displayed. As expected, due to the equality between macroscopic and mesoscopic stress fields and to $c \ll E$, mesoscopic plastic strains in the inclusion are very important (6%), which is not realistic, and we can conclude that the Sachs scheme is not appropriate for this type of loading.

Fig. 2 presents the differences between Lin-Taylor's and Kröner's schemes. One can remark that the stress-strain curves are similar, with a factor of two on the plastic dissipated energy value. However, the mesoscopic residual stresses are completely different. For the Lin-Taylor scheme, the dissipation due to the residual stresses, $d_{\text{res}} = -2\mu\boldsymbol{\varepsilon}^p : \dot{\boldsymbol{\varepsilon}}$, is negative and has a larger absolute value than the plastic dissipation $d_p = \boldsymbol{\sigma} : \dot{\boldsymbol{\varepsilon}}_p$. As a consequence the mean temperature of the cycle will decrease with growing number of cycles as shown in Fig. 3. The temperature decrease predicted with the Lin-Taylor model is in contradiction with experimental observations (see, for example, Fargione et al. [6]). We can conclude that only Kröner's homogenization scheme permits the obtainment of consistent qualitative results, as proven by the studied example displayed in Fig. 3. The quantitative predictions are cyclic temperature amplitude of ≈ 0.3 K (see Fig. 4) and a mean temperature increase of about 0.5 K which is in the order of magnitude of the experimental observations.

A direct comparison of the numerical prediction of the mean temperature increase with respect to the applied load amplitude with experiments of Boulanger [7] is presented in Fig. 5. A good match between predictions and experiments can be observed for low level of loadings. The quality of the match is decreasing with increasing loading. This can be explained by the hypothesis of a simple slip system which is very restrictive and certainly not representative of the local behaviour.

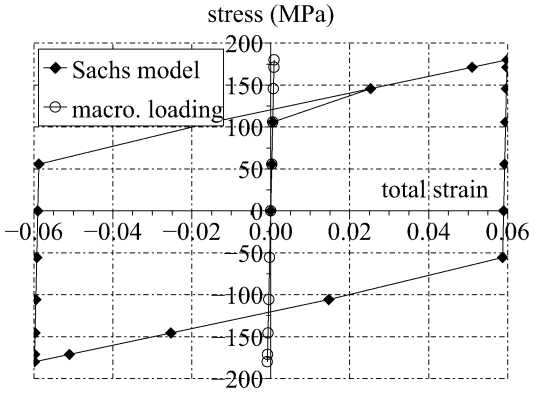

Fig. 1. Stress-strain curves corresponding to the elastic macroscopic loading and to the mesoscopic response for the Sachs scheme.

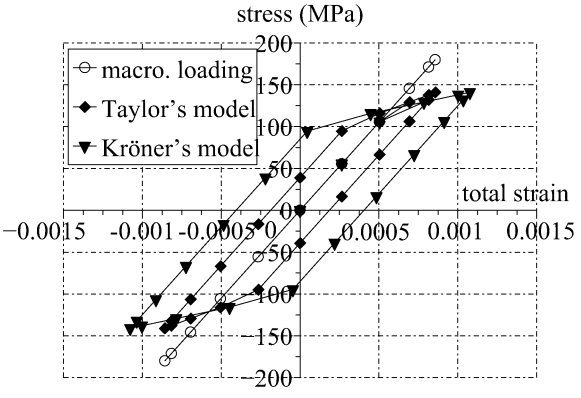

Fig. 2. Stress-strain curves corresponding to the elastic macroscopic loading and to the mesoscopic responses for the Kröner's and Taylor's schemes.

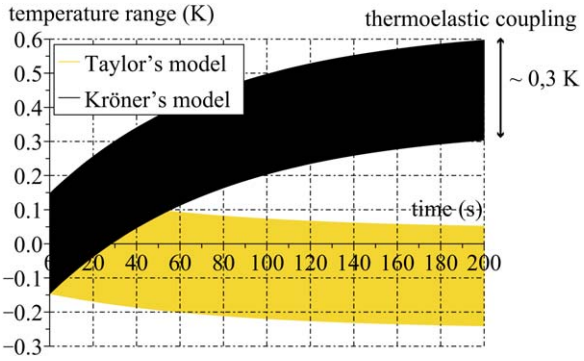

Fig. 3. Evolution of the temperature range during cyclic loading for the Kröner's and Taylor's schemes for a stress amplitude of 180 MPa.

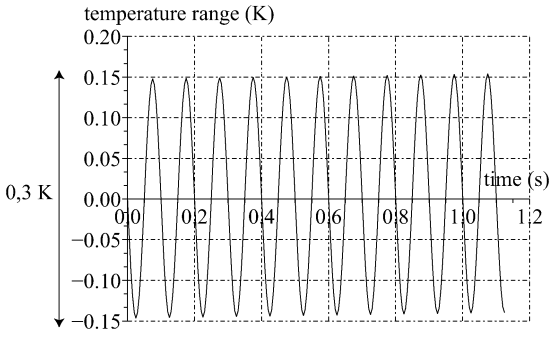

Fig. 4. Evolution of the temperature range during the first 10 cycles for the Kröner's scheme: the sinusoidal response is due to the thermoelastic coupling.

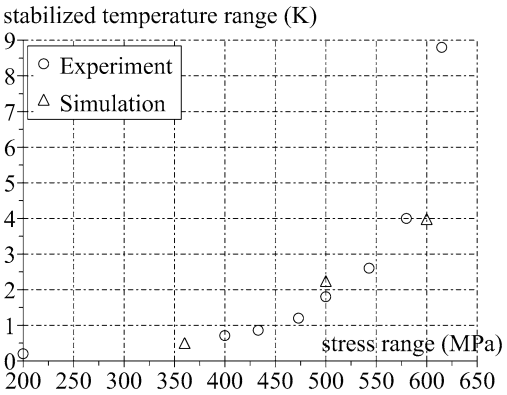

Fig. 5. Evolution of the stabilized mean temperature with respect to the loading amplitude. The experimental results stem from Boulanger [7].

5. Conclusion

A series of High-Cycle Fatigue (HCF) criteria for polycrystalline materials have been developed using a multiscale model, and based on a shakedown condition for defining the fatigue limit. In this Note, the study of the different dissipative regime during cyclic loading were extended within this framework by using a self consistent homogenization scheme in coupled thermoplasticity. It is shown that the Sachs and Lin-Taylor schemes are not able to represent the thermal evolutions observed during fatigue tests. Kröner's scheme is in good qualitative accordance with the experimental results (thermoelastic coupling, plastic dissipation). Moreover, the proposed model was able to predict quantitatively mean temperature measurements provided by Boulanger [7]. A refinement of the local thermal and mechanical behaviors should permit to further validate this approach.

Appendix A. Incremental thermomechanical problem

The heat balance equation which has to be solved corresponds to Eq. (5). The simplest solution to solve such an equation consists in a numerical integration. The mesoscopic plastic strain increment $\Delta\boldsymbol{\varepsilon}^p$ has to be first determined. The algorithm used for the elastoplastic step follows an implicit radial return technique (see, for example, [14]), which gives explicitly, in the case of a purely linear hardening law, the expression of the plastic strain increment as a function of the total strain increment:

$$\Delta\boldsymbol{\varepsilon}^p = \frac{\sqrt{\frac{3}{2}}\|\boldsymbol{A}^*_{n+1}\| - \sigma_y}{\sqrt{\frac{3}{2}}(2\mu - 2\mu b + c)\Delta t}\frac{\boldsymbol{A}^*_{n+1}}{\|\boldsymbol{A}^*_{n+1}\|} \tag{A.1}$$

where $\boldsymbol{A}^*_{n+1}$ corresponds to the deviatoric trial stress, defined, for a purely elastic strain increment, by $\boldsymbol{A}^*_{n+1} = \mathbb{K} : \mathbb{C} : \boldsymbol{\varepsilon}_n - (2\mu - 2\mu b + c)\boldsymbol{\varepsilon}^p_n + \mathbb{K} : \mathbb{C} : \Delta\boldsymbol{\varepsilon}$.

For the thermal differential equation (5), an explicit time integration is used and the incremental translation of Eq. (5) is then the following:

$$T_{n+1} = \frac{\frac{T_n}{\Delta t} + \frac{T_0}{\tau_{\text{eq}}} + \frac{f_v}{\rho C_v \Delta t}(\boldsymbol{\sigma}_n : \Delta\boldsymbol{\varepsilon}^p - \frac{2}{3}c\boldsymbol{\varepsilon}^p_n : \Delta\boldsymbol{\varepsilon}^p - (2\mu - 2\mu b)\boldsymbol{\varepsilon}^p_n : \Delta\boldsymbol{\varepsilon})}{\frac{1}{\Delta t} + \frac{1}{\tau_{\text{eq}}} + \frac{\alpha}{\rho C_v \Delta t}\,\text{tr}(\Delta\boldsymbol{\Sigma})} \tag{A.2}$$

References

[1] K. Dang Van, I.V. Papadopoulos, in: K. Dang Van, I.V. Papadopoulos (Eds.), High-Cycle Metal Fatigue, From Theory to Applications, in: CISM Courses and Lectures, vol. 392, Springer-Verlag, Berlin/New York, 1999.

[2] M. Bornert, T. Bretheau, P. Gilormini, Homogénéisation en Mécanique des matériaux, Tome 2, Comportements non linéaires et problèmes ouverts, Hermes Science, 2001.

[3] J. Mandel, J. Zarka, B. Halphen, Adaptation d'une structure élastoplastique à écrouissage cinématique, Mech. Res. Commun. 4 (1977) 5.

[4] Q.S. Nguyen, On shakedown analysis in hardening plasticity, J. Mech. Phys. Solids 51 (2003) 101–125.

[5] M.P. Luong, Infrared thermographic scanning of fatigue in metals, Nuclear. Engrg. and Design 158 (1995) 363–376.

[6] G. Fargione, A. Geraci, G. La Rosa, A. Risitano, Rapid determination of the fatigue curve by the thermographic method, Internat. J. Fat. 24 (2002) 11–19.

[7] T. Boulanger, A. Chrysochoos, C. Mabru, A. Galtier, Calorimetric analysis of dissipative and thermoelastic effects associated with the fatigue behavior of steels, Internat. J. Fat. 26 (2004) 221–229.

[8] C. Doudard, Détermination rapide des propriétés en fatigue à grand nombre de cycles à partir d'essais d'échauffement, Thèse de Doctorat de l'Ecole Normale Supérieure de Cachan, spécialité : Mécanique, 2004.

[9] C. Doudard, S. Calloch, P. Cugy, A. Galtier, F. Hild, A probabilistic two-scale model for high-cycle fatigue life predictions, Fatigue Fract. Engrg. Mater. Struct. 28 (2005) 279–288.

[10] F. Cano, A. Constantinescu, H. Maitournam, Critère de fatigue polycyclique pour des matériaux anisotropes : application aux monocristaux, C. R. Mécanique 332 (2004) 115–121.

[11] J. Lemaitre, J.L. Chaboche, Mécanique des matériaux solides, Dunod, 1985.

[12] V. Monchiet, E. Charkaluk, D. Kondo, A plasticity-damage based micromechanical modelling in high cycle fatigue, C. R. Mécanique 334 (2006) 129–136.

[13] P. Cugy, A. Galtier, Microplasticity and temperature increase in low carbon steels, in: A.F. Blom (Ed.), Fatigue 2002, EMAS, 2002, pp. 549–556.

[14] J.C. Simo, T.J.R. Hughes, Computational Inelasticity, Springer-Verlag, Berlin/New York, 1998.

[15] A. Chrysochoos, H. Louche, An infrared image processing to analyse the calorific effects accompanying strain localisation, Internat. J. Engrg. Sci. 38 (2000) 1759–1788.